Article

Crosstalk of non-apoptotic RCD panel in hepatocellular carcinoma reveals the prognostic and therapeutic optimization

Liver cancer cell death process regulated by multiple RCD genes

Poor prognosis → Good prognosis

Tumor subtype

TIME — Genomics alterations — Epigenetics differences — Biological function — Gene Panel

Therapy analysis — Immunohistochemistry staining — qRT-PCR

Shuo Li, Yaqi Xu, Xin Hu, ..., Chunhui Yuan, Chen Liang, Fubing Wang

sywj0928@126.com (J.W.)
chunhuii.yuen@whu.edu.cn (C.Y.)
zn001138@whu.edu.cn (C.L.)
wfb20042002@sina.com (F.W.)

Highlights

Non-apoptotic RCD played a key role in HCC progression and prognosis

The RCDRS scoring panel was established for risk assessment of HCC patients

RCDRS shows potential in predicting chemotherapy drugs treatment efficacy

RCDRS demonstrates predictive value in immunotherapy for HCC patients
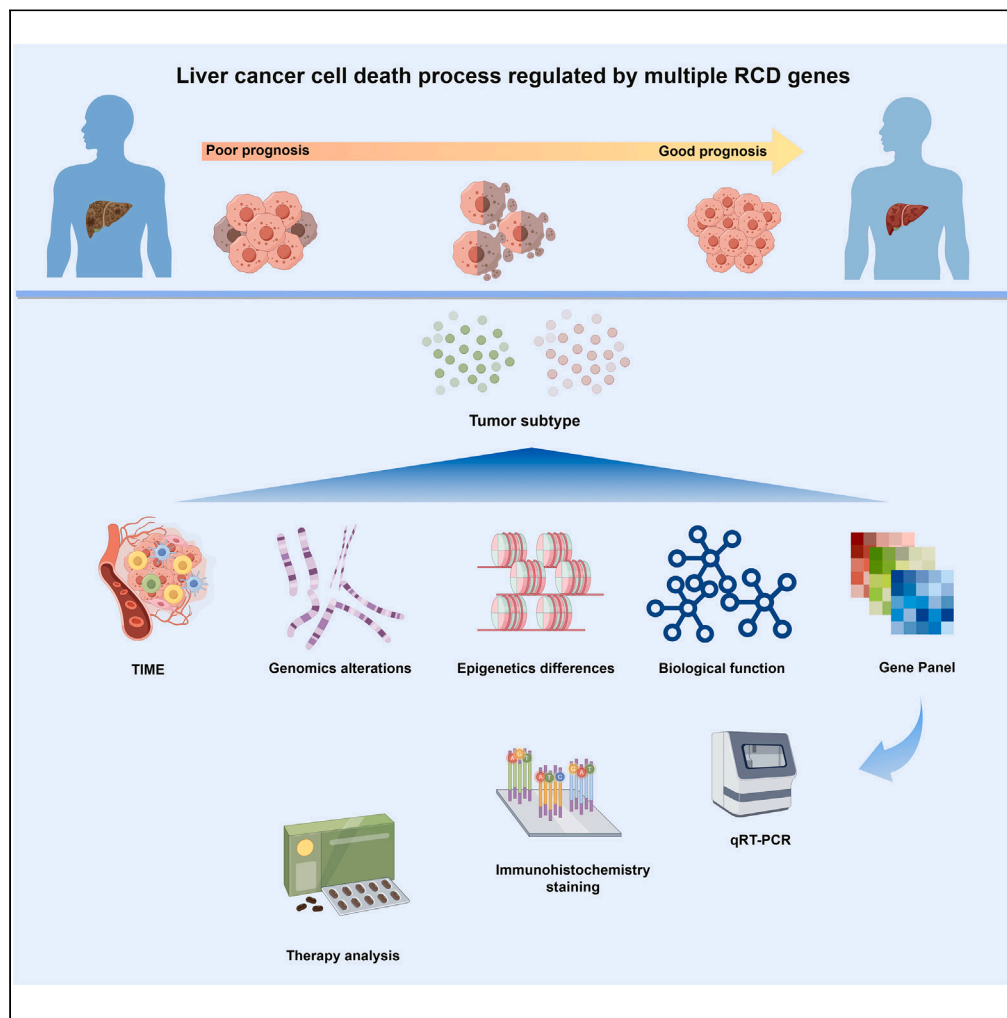
iScience

Article

Crosstalk of non-apoptotic RCD panel in hepatocellular carcinoma reveals the prognostic and therapeutic optimization

Shuo Li,[1,2,8] Yaqi Xu,[1,2,8] Xin Hu,[1,2,8] Hao Chen,[3,8] Xiaodan Xi,[1,2] Fei Long,[1,2] Yuan Rong,[4,2] Jun Wang,[5,*] Chunhui Yuan,[5,2,*] Chen Liang,[6,*] and Fubing Wang[1,2,7,9,*]

SUMMARY

Non-apoptotic regulated cell death (RCD) of tumor cells profoundly affects tumor progression and plays critical roles in determining response to immune checkpoint inhibitors (ICIs). Prognosis-distinctive HCC subtypes were identified by consensus cluster analysis based on the expressions of 507 non-apoptotic RCD genes obtained from databases and literature. Meanwhile, a set of bioinformatic tools was integrated to analyze the differences of the tumor immune microenvironment infiltration, genetic mutation, copy number variation, and epigenetics alternations within two subtypes. Finally, a non-apoptotic RCDRS signature was constructed and its reliability was evaluated in HCC patients' tissues. The high-RCDRS HCC subgroup showed a significantly lower overall survival and less sensitivity to ICIs compared to low-RCDRS subgroup, but higher sensitivity to cisplatin, paclitaxel, and sorafenib. Overall, we established an RCDRS panel consisting of four non-apoptotic RCD genes, which might be a promising predictor for evaluating HCC prognosis, guiding therapeutic decision-making, and ultimately improving patient outcomes.

INTRODUCTION

Hepatocellular carcinoma (HCC), a prevalent type of primary liver cancer worldwide, is characterized by notable intratumoral heterogeneity, the acquisition of therapeutic resistance, and a dismal prognosis.[1] Although early-stage disease may be curable by the expanding implementation of surgical, locoregional, and transplantation therapies, most HCC patients presenting with unresectable disease (50–60%) will ultimately be treated with systemic therapies.[2]

The emergence of immune checkpoint inhibitors (ICIs) has completely revolutionized the systemic management of HCC, and multi-pronged approaches involving the combination of ICIs with additional targeted agents are currently being tested to improve outcomes of HCC patients.[3,4] Significantly, the combination of the anti-PD-L1 atezolizumab and the anti-VEGF bevacizumab has become the preferred first-line therapy according to the latest National Comprehensive Cancer Network (NCCN) clinical practice guidelines for hepatobiliary cancers (Version 1. 2022).[5] However, the objective response rates (ORRs) of HCC were only approximately 35% after combination treatment.[6] There still more than half of the patients did not derive benefit, and hyperprogressive disease (accelerated tumor growth) has been further described in 12.7% of HCC patients following received PD-1/PD-L1-targeted ICIs.[2] Thus, precise, and accurate predictive biomarkers that could be utilized for optimal integration of ICIs-based combination to maximize the efficacy is urgently needed in HCC patients.

Response to ICIs-based therapies can be determined by multiple factors, like mutational, transcriptomic, and epigenetic alterations, as well as the fundamental tumor immune microenvironment (TIME).[5,7] The three clinical approved biomarkers, including tumor mutation burden (TMB) and microsatellite instability (MSI) that closely linked to neoantigen load and expression of PD-L1 in tumor or immune cells, have been confirmed to be significantly associated with ICIs-based responses in multiple tumor types.[2] However, these biomarkers have limited predictive value due to the low prevalence of high TMB, microsatellite instability (<1%), or PD-L1 expression (cutoff $\geq$1%) in

[1]Department of Laboratory Medicine, Zhongnan Hospital of Wuhan University, Wuhan 430071, China
[2]Center for Single-Cell Omics and Tumor Liquid Biopsy, Zhongnan Hospital of Wuhan University, Wuhan 430071, China
[3]Department of Pathology, Zhongnan Hospital of Wuhan University, Wuhan 430071, China
[4]Forensic Center of Justice, Zhongnan Hospital of Wuhan University, Wuhan China
[5]Department of Laboratory Medicine, Wuhan Children's Hospital (Wuhan Maternal and Child Healthcare Hospital), Tongji Medical College, Huazhong University of Science & Technology, Wuhan 430016, China
[6]Department of Radiation and Medical Oncology, Zhongnan Hospital of Wuhan University, No. 169 Donghu Road, Wuchang District, Wuhan 430071, China
[7]Wuhan Research Center for Infectious Diseases and Cancer, Chinese Academy of Medical Sciences, Wuhan, China
[8]These authors contributed equally
[9]Lead contact
*Correspondence: sywj0928@126.com (J.W.), chunhuii.yuen@whu.edu.cn (C.Y.), zn001138@whu.edu.cn (C.L.), wfb20042002@sina.com (F.W.)
https://doi.org/10.1016/j.isci.2024.109901

HCC.[8] In the dose-expansion phase of multicohort trial CheckMate 040 (NCT01658878), PD-L1 positivity of less than 1% was observed in 140 of 174 HCC patients and did not have an apparent difference in ORR compared to PD-L1 expression greater than 1% (26/140 vs. 9/34).[9] Thus, the development of highly effective ICIs-based therapies remains limited by the lack of validated predictors that can be used in the treatment of routine HCC patients.

ICIs-based therapies mainly act by reinvigorating tumor-immune interactions, and thus renewed interest has been focused on immune-related signatures as a means of predicting response in HCC. An inflammatory 4-gene signature was shown to associate with improved survival and nivolumab's response in dose-escalation and -expansion phases of CheckMate 040.[10] Similarly, an 11-gene signature including genes involved in infiltration of M1 macrophages and CD4$^+$ T cells was predictive of anti-PD1 response in patients with HCC,[11] while which was not able to identify responders among HCC patients that were pre-treated with tyrosine kinase inhibitors (TKIs).

Recently, many studies have confirmed that non-apoptotic regulated cell death (RCD) of tumor cells profoundly affects the progression, TIME infiltration, and thus plays critical roles in determining response to ICIs.[12–14] Autophagy, ferroptosis, pyroptosis, necroptosis, and the newly emerging cuproptosis all belonged to the subtypes of non-apoptotic RCD.[15] Notably, the type of non-apoptotic RCD executed not only affects the lineage commitment in liver tumorigenesis,[16] but also has double-edged sword effects for therapeutic responses in HCC.[17–20] Therefore, the establishment of a predictive panel that incorporates non-apoptotic RCD may have profound implications for maximizing benefit of ICIs-based therapies in HCC patients.

Here, we systematically analyzed the differences in biological functions, TIME characteristics, mutation patterns and epigenetic alternations between the two clusters of HCC patients based on non-apoptotic RCD genes classification. Meanwhile, we identified four key non-apoptotic RCD genes and established a promising quantitative risk scores panel. Moreover, the reliability and accuracy of the panel were verified by tissue samples and cohorts. These findings imply that the panel holds significant prognostic value and can be utilized to enhance precision therapy for HCC patients, ultimately resulting in improved patient survival.

RESULTS

Two distinct HCC subtypes mediated by non-apoptotic RCD genes

We extracted 507 non-apoptotic RCD genes from published literature[15] and performed consensus cluster analysis on 368 samples with complete survival information screened from the TCGA database, and the results were shown non-apoptotic RCD genes could well classify HCC patients into cluster1 (*N* = 177) and cluster2 (*N* = 191) groups (Figure 1A), and the cumulative distribution function (CDF) curves confirmed the classification effect was the best (Figure 1B). Also we summarized the relationship between RCD subtypes and clinical indexes in TCGA LIHC cohort (Table S1). To further evaluate the classification accuracy of these two clusters, principal components analysis (PCA) was performed and showed a clear grouping division for two clusters (Figure 1C), which was further confirmed the two clusters are different. Heatmap results of non-apoptotic RCD genes expression and clinical characteristics in HCC patients also showed that its expression was significantly different from two clusters (Figure 1D). Comparing the survival probabilities, it was observed that the cluster 2 group had significantly better overall survival as compared to the cluster 1 group. (Figure 1E). Taken together, our results provided preliminary evidence of the prognostic values of non-apoptotic RCD in HCC patients. Furthermore, we compared the differences between the two subtypes in terms of biological characteristics and prognostic signature (Figure S1).

Differentially biological function and TIME characteristics in two cluster subtypes

To gain a deeper understanding of the contrasting biological functions between the two clusters, GSVA enrichment analysis was performed. The analysis revealed that cluster 1 exhibited an enrichment in the activation of cell proliferation-related signaling pathways, including the mitotic spindle and G2M checkpoint signaling pathways. Conversely, cluster 2 showed enrichment in the inhibition of KRAS signaling, as well as pathways associated with coagulation and xenobiotic metabolism. (Figure 2A). A basically consistent results was observed in GSEA KEGG (Figure S2) and GO (Figure S3) analyses. To further observe the TIME characteristics between the two clusters, we performed a score analysis of the infiltration of 28 types of immune cells in the HCC microenvironment, and showed that the cluster 1 had a relatively higher immune score (Figure 2B). Infiltrating abundance analysis further showed that the relative infiltration abundance of 11 types immune cells (such as T cells CD4 memory resting, T cells CD4 memory activated and T cells CD4 naive) was significant higher in cluster 1 (Figure 2C). Therefore, these results further implied that non-apoptotic RCD was closely associated to tumor proliferation, metabolism, and other cancer related pathways, and had synergistic or antagonistic effects with immune cell infiltration in TIME.

Significant differences of mutation pattern in two cluster subtypes

To investigate the mutation patterns between the two clusters and their association with non-apoptotic RCD, we firstly performed significantly mutation genes (SMG) analysis based on the TCGA-LIHC cohort, the gene mutation ratio between the two clusters were shown by waterfall plots, we could clearly see that several SMGs including TP53, ALB, OBSCN, and SPTA1 in cluster 1 had more significant mutations compared with cluster 2 (Figure 3A). Based on the Catalogue of Somatic Mutations in Cancer database (COSMIC database: https://cancer.sanger.ac.uk/signatures/signatures_v2/) revealed that the process of mutation operation of the cluster 1 group mainly showed signature 3 and 12 characteristics, but the cluster 2 group mainly showed signature 4 and signature 16 characteristics. (Figures 3B and 3C). Therefore,
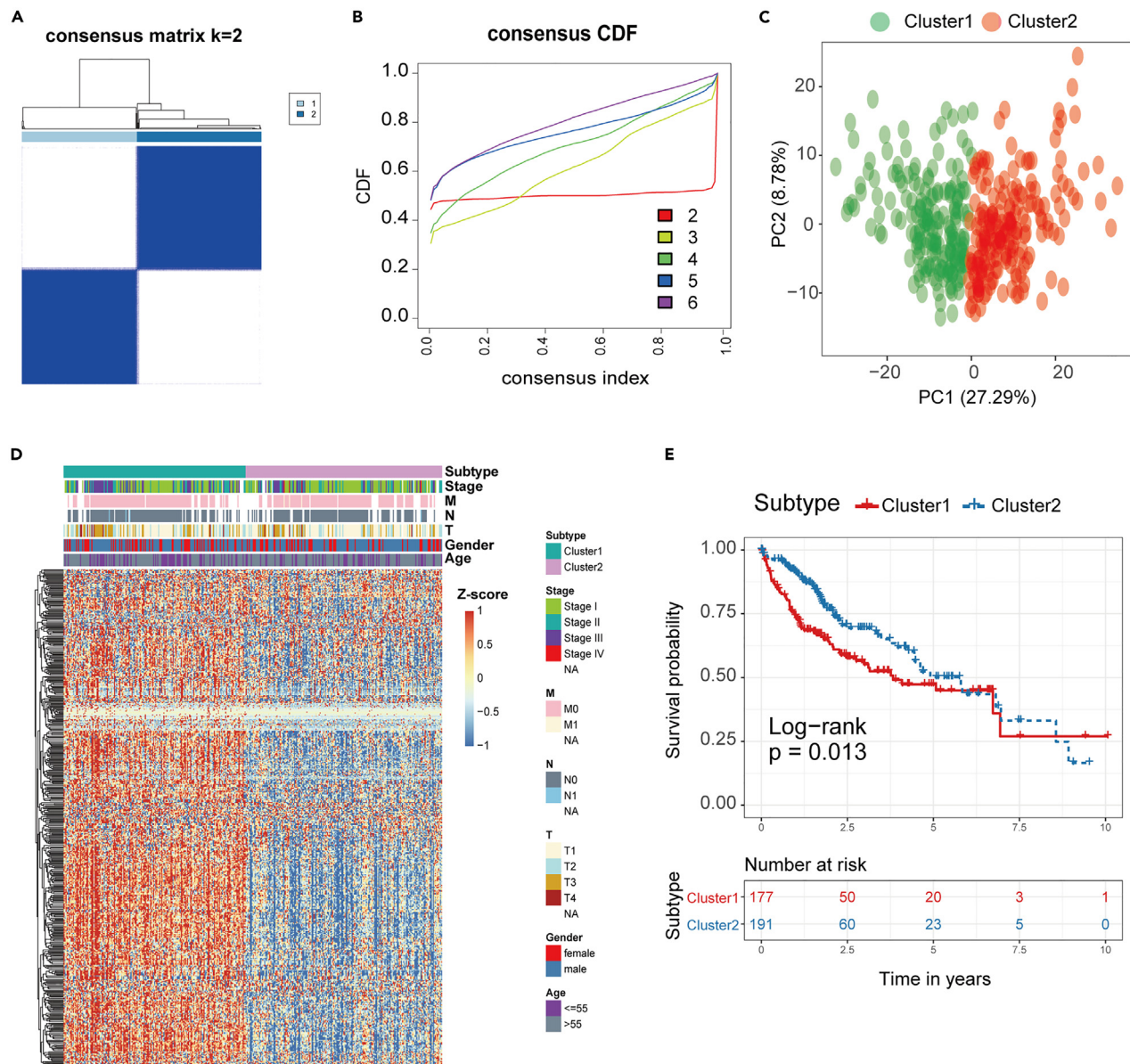
Figure 1. Non-apoptosis RCD genes cluster analysis classified HCC patients into two distinct subtypes

(A and B) The optimal number of clusters (K = 2) was determined from cumulative distribution function (CDF) curves, and the classification effect is the best.

(C) Principal component analysis (PCA) plot of GC samples.

(D) The patients were divided into two groups: Cluster1 and Cluster2. The RCD gene expression was normalized into Z score.

(E) Survival analysis of three RCD subtypes in the TCGA LIHC cohort was created using Kaplan-Meier curves. *$p < 0.05$.

these results indicated that HCC patients could be well divided into two clusters based on non-apoptotic RCD classification, and the two clusters had their own distinctive gene mutation patterns.

Epigenetics differences between the two cluster subtypes

Resolving the epigenetic landscape of cancer cells is not only critical for a precise understanding of cancer etiology and progression, but also has important implications for the potential development of cancer therapeutics.[21] Here, we first analyzed the differential CNV alterations between the two clusters, the results showed significant differences, for example, cluster 1 had many copy-number deletions (e.g., 1p36.11, 4q21.3, 4q24, 4q35.1, and 14q23.3) and a small number of copy-number amplifications (1q21.3, 5q35.3, and 6p25.2) (Figure 4A). In addition, the cluster1 group showed the highest overall burden of copy number gain and copy number loss. Moreover, further focal and arm level CNV analyses also revealed that the cluster1 group showed the higher level of copy number
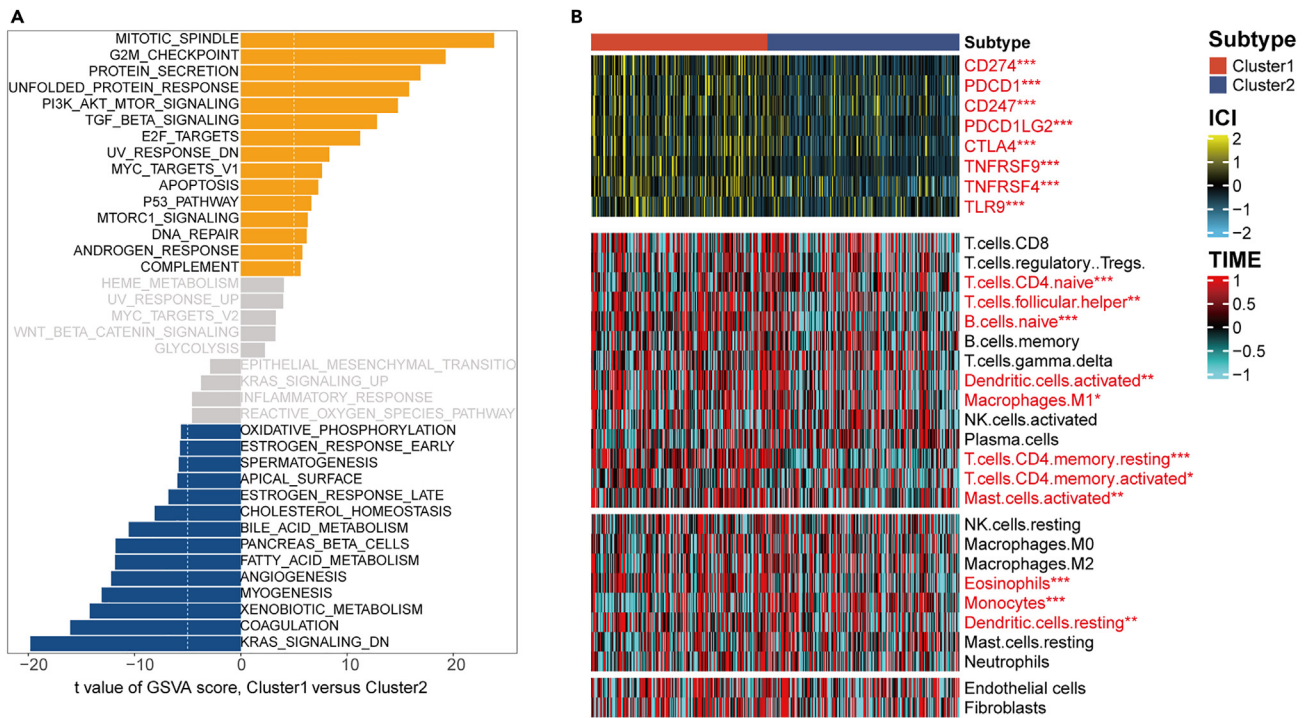
Figure 2. Biological function and TIME characteristics of different RCD clusters in TCGA cohort

(A) The GSVA plot showed a differentially activated pathway between the two clusters. Each yellow bar showed an activated pathway, and each blue bar showed an inactivated pathway. (|t value| > 5 and $p < 0.05$).

(B) The relative infiltration of each immune cell type and the expression of immune checkpoints were normalized into Z score. $*p < 0.05$, $**p < 0.01$, $***p < 0.001$.

gain and loss (Figure 4B). In additional, analysis of the methylation driver genes in TCGA-LIHC by MethylMix package also showed that up to 24 methylation driver genes were significantly different between the two clusters (Figure 4C). And this difference is reflected not only in the level of methylation modification (Figure 4D), but also in their own mRNA expression (Figure 4E). These results further indicated that there was a close relationship between epigenetic alteration and non-apoptotic RCD in HCC patients.

RCDRS was established as an independent prognostic biomarker

With the above confirmation that HCC patients can be well divided into two cluster groups based on non-apoptotic RCD genes, we attempted to further constructing an expression pattern score that can accurately quantify individual tumor patients. 1188 genes from TCGA-LIHC cohort and 507 non-apoptotic RCD genes from literature were analyzed, the significantly gene (|log2FC| >1 & $p < 0.05$) expression levels in two clusters were presented by volcano plots (Figure 5A). Univariate Cox and lasso Cox regression analysis showed that nine genes had significant prognostic significance (Figures 5B and 5C). Further stepwise multiple regression analysis showed that PLOD2, G6PD, FTCD and ADH4 were the four most significant valuable genes in non-apoptotic RCD classification of HCC patients (Table S2). Meanwhile, heatmap analysis also showed that the expression of these four genes was highly correlated with the HCC patients clinical characteristics, among which cluster 1 was mainly highly expressed with PLOD2 and G6PD, but cluster2 was mainly highly expressed with FTCD and ADH4 (Figure 5D). And based on these findings, we established a prognostic panel that effectively classified HCC patients, as follows: RCDRS score = 0.2426 × exp (PLOD2) + 0.1833 × exp (G6PD) - 0.0855 × exp (FTCD) - 0.0508 × exp (ADH4). The results revealed the high-RCDRS group had a markedly lower survival probability than that the low-RCDRS group (Figure 5E), and cut-off value calculated by the R package survminer was 1.0239. The accuracy of the panel for HCC prognosis was verified by ROC analysis, the AUC of 3- and 5-year survival predictive was 0.716 and 0.679, respectively (Figure S4). Kaplan–Meir analysis showed that similar significant results into GEO cohort: GSE116174 (Figure S5). As shown by multivariate Cox regression analysis, RCDRS was a remarkably independent predictor with higher indicating a worse prognosis (Figure 5F).

What's more, the nomogram of independent factors (age, gender, stage, and RCDRS) also revealed the same findings (Figure 5G). The calibration curve further indicated a well predicted and prognostic observations at 3- and 5-year OS in TCGA cohort (Figure S6). These results illustrated that our prognostic risk panel (RCDRS) could effectively classify HCC patients into high and low risk groups.

Validation of the four non-apoptotic RCD genes in clinical tissues

To further investigate the role of the four non-apoptotic RCD genes in HCC patients, we performed real-time quantitative PCR (RT-qPCR) to assess their expression levels in both HCC and adjacent normal tissues. The results demonstrated significantly higher relative expression
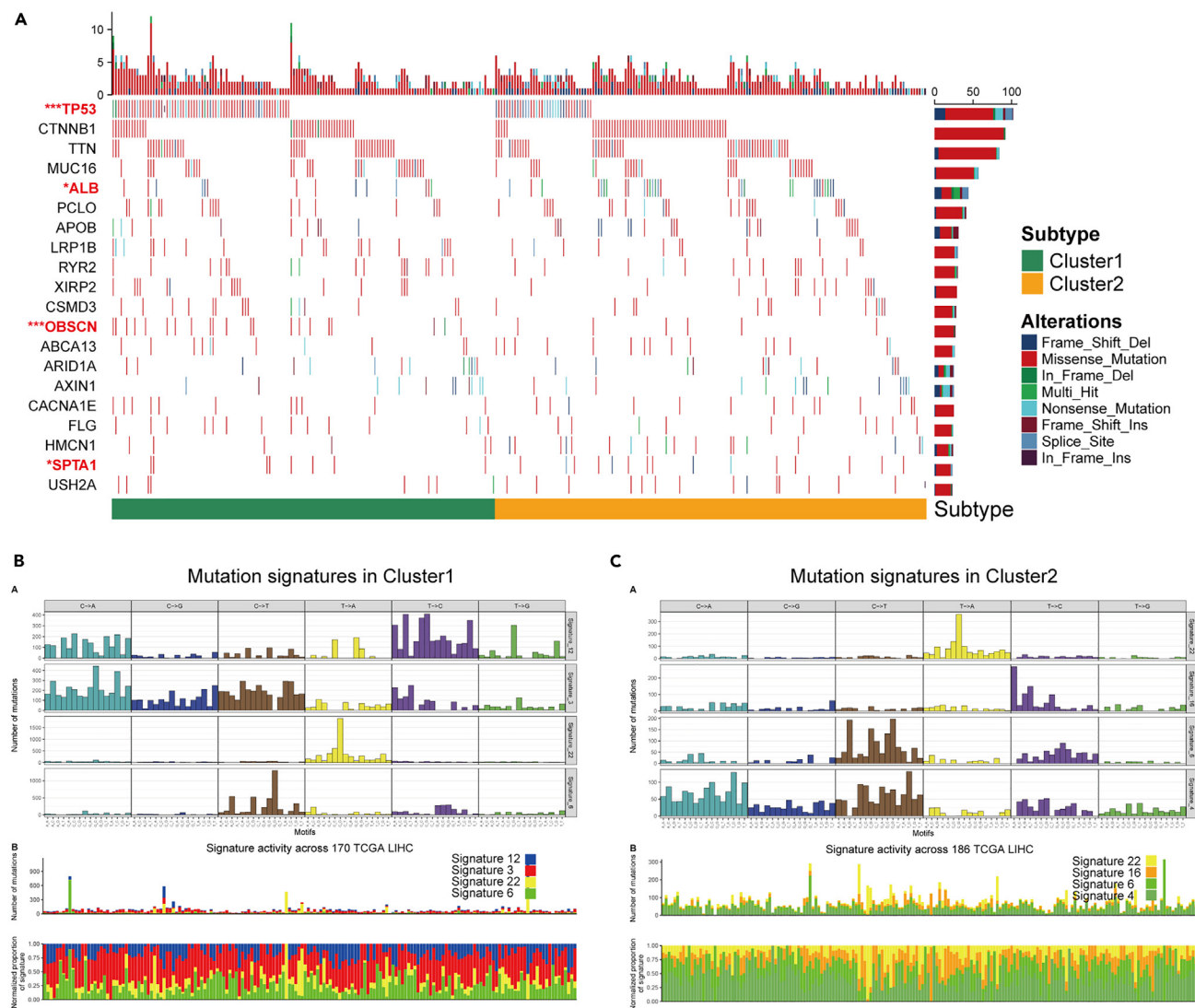
Figure 3. Mutational landscape in two clusters
(A) Mutational landscape of gene between two RCD subtypes.
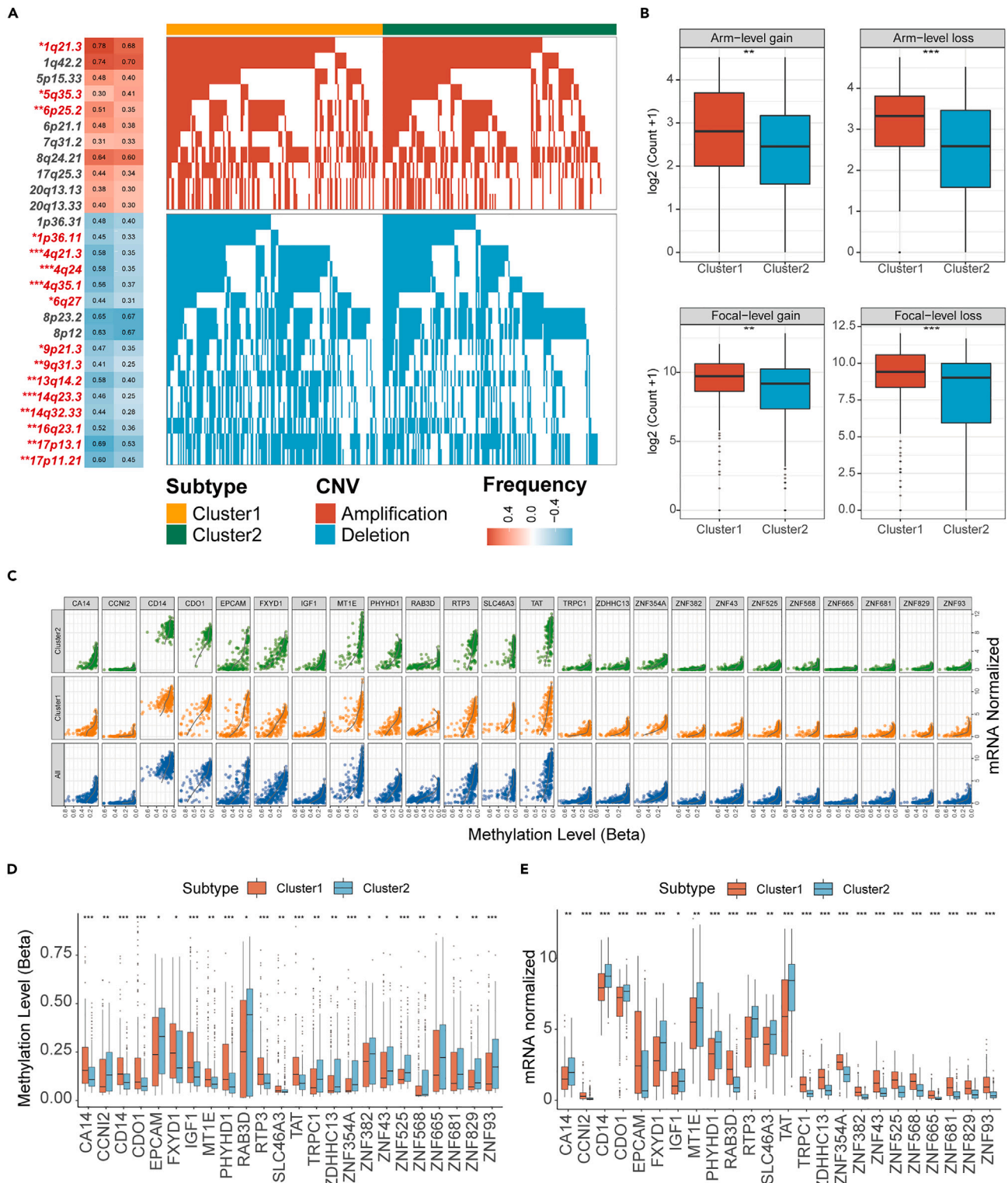(B) Mutation signatures in cluster 1.
(C) Mutation signatures in cluster 2. *$p < 0.05$, **$p < 0.01$, ***$p < 0.001$.

levels of PLOD2 and G6PD in HCC tissues than in adjacent normal tissues, while the opposite trend was observed for FTCD and ADH4 (Figure 6A). Immunohistochemical staining was performed to validate the expression in protein level, coincidentally, there were consistent with the above (Figure 6B). Moreover, multiplexed immunofluorescence staining further confirmed that PLOD2 and G6PD were higher expression in HCC tissues, and FTCD and ADH4 were mainly verified accumulated in adjacent normal tissues (Figure 6C). In conclusion, our tissue validation results were highly consistent with the bulk RNA sequence, further indicating that the panel based on the four non-apoptotic RCD genes could be used to distinguish HCC progression effectively.

The predictive value of RCDRS in chemotherapy drugs selection and response in two risk groups

Given the critical role of non-apoptotic RCD genes in HCC progression, we further evaluated the predictive value of RCDRS in optimizing potential drugs selection and response to drug therapy in the TCGA-LIHC cohort. eXtreme Sum (XSum) algorithm analysis showed that the small molecule drug STOCK1N. 35696 was the potential therapeutic agent that could benefit patients in high-RCDRS group (Figure 7A). Prediction of response to conventional chemotherapy drugs for HCC by the R package pRRophetic showed that high-RCDRS groups had the lower estimated IC50 for cisplatin, paclitaxel and sorafenib (Figures 7B, 7C, and 7D). This indicated that RCDRS can be used to optimize appropriate chemotherapy drugs for patients with HCC.
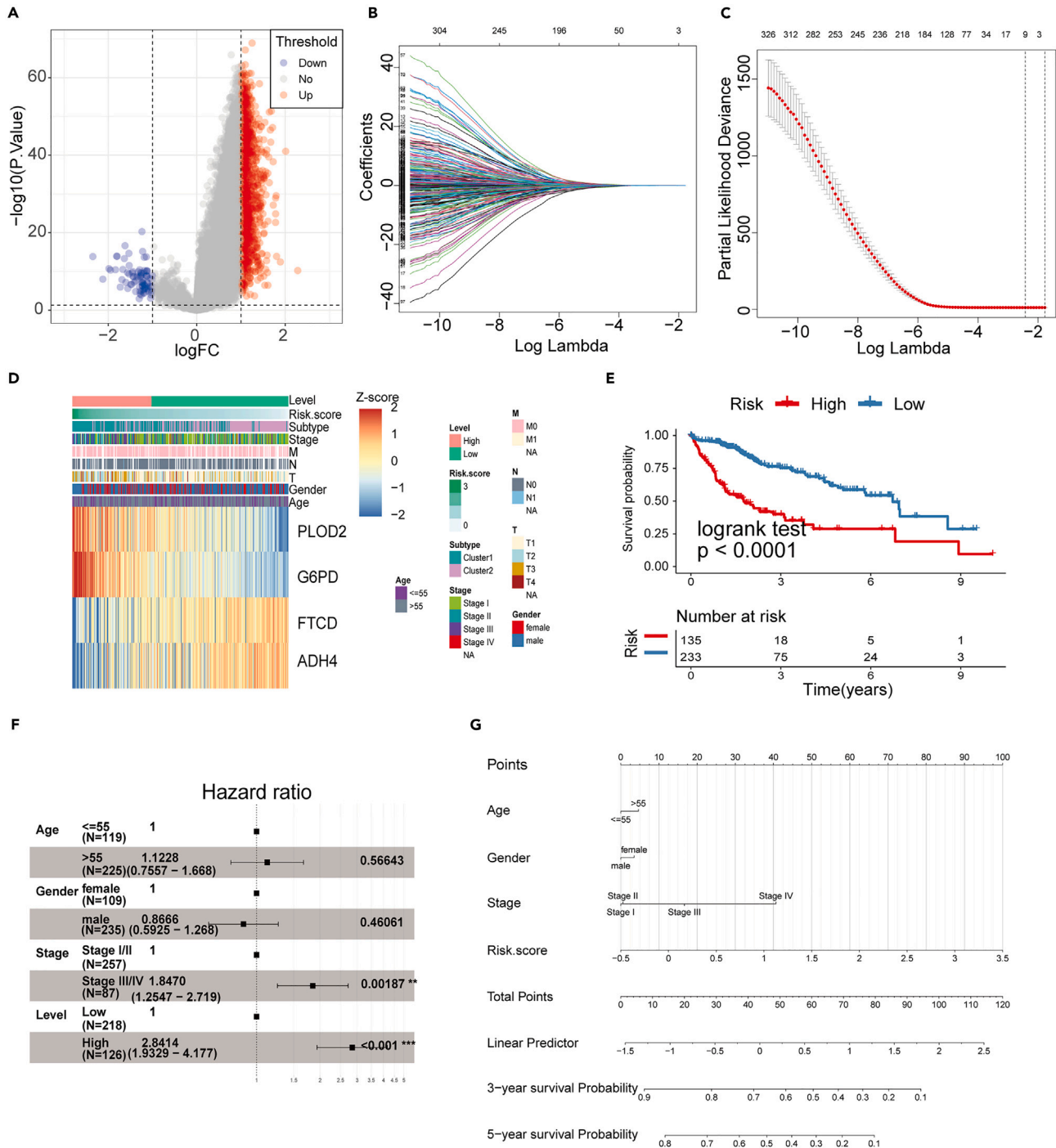
Figure 4. Epigenetic alternations in two clusters

(A) Detailed plots with copy number amplifications and deletions between two RCD subtypes.

(B) Distribution of focal and broad copy number alterations (gain and loss) between two RCD subtypes.

(C) The correlation of Beta value and gene expression based on 24 methylation driven genes.

(D and E) The boxplot showed that methylation driven genes in different RCD subtypes. $*p < 0.05$, $**p < 0.01$, $***p < 0.001$. Data are represented as mean (SD).

Figure 5. Identification of non-apoptosis RCD-related signatures (RCDRS) in LIHC

(A) The volcano plot showed that 1188 differentially expressed mRNAs and 507 non-apoptosis RCD genes between Cluster1 and Cluster2 subtypes. Red dots indicated significant up-regulated of mRNA expression, blue dots indicated significant down-regulated of mRNA expression, and gray dots indicated no significant changes of mRNA expression.

(B and C) LASSO variables screening process.

(D) Survival analysis of RCDRS in the TCGA-LIHC cohort was created using Kaplan-Meier curves.

(E) Multivariate Cox regression analyses of the association between clinicopathological factors and OS of LIHC patients in TCGA cohort.

(F) The expression of four mRNAs in LIHC patients.

(G) The nomogram consists of the clinical characteristics (age, sex, stage) and risk score. The variable scores were summed to give the total points, and the total point line is shown at the bottom of the nomogram. *$p < 0.05$, **$p < 0.01$, ***$p < 0.001$.
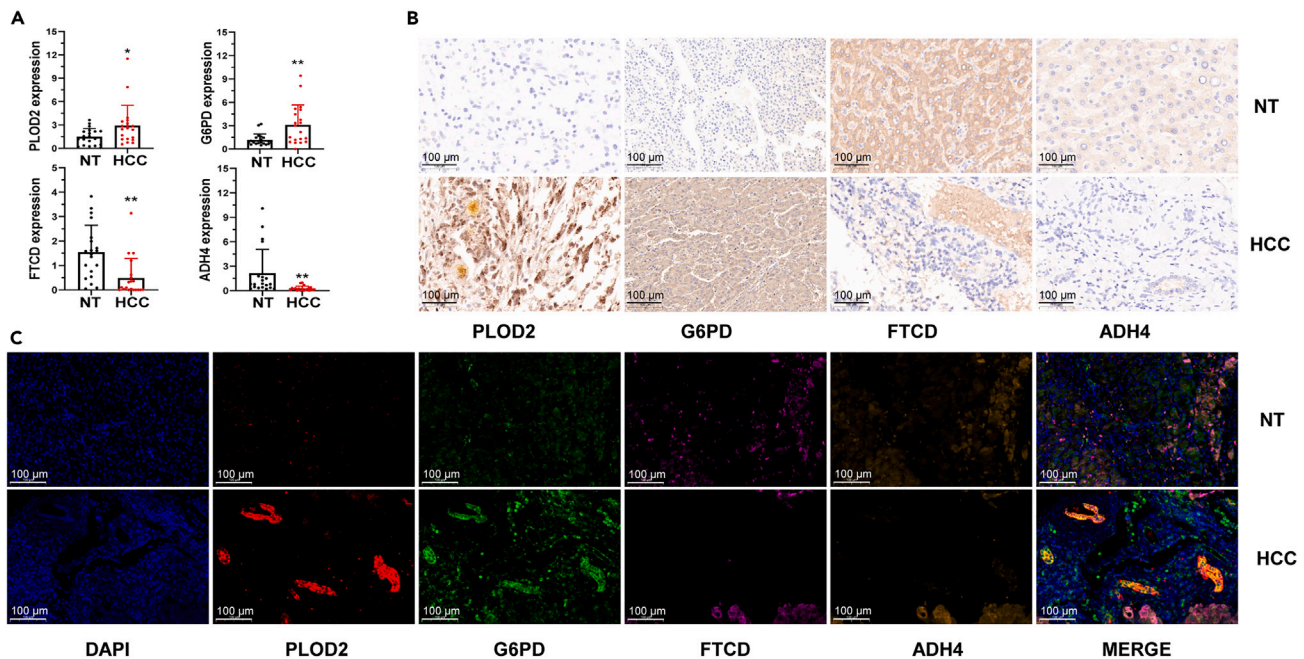
Figure 6. Validation of the four non-apoptotic RCD genes in clinical tissues
(A) qRT-PCR of PLOD2, G6PD, FTCD and ADH4 relative expression in adjacent normal tissues (NT) and HCC tissues, the relative expression was normalized to GAPDH. *$p < 0.05$, **$p < 0.01$.
(B) Immunohistochemical staining showed the protein expression of PLOD2, G6PD, FTCD and ADH4 in adjacent normal tissues (NT) and HCC tissues. The nuclei were stained with in blue and the positive cells were stained with brown.
(C) Multiplexed immunofluorescence staining showed the expression and location of PLOD2, G6PD, FTCD and ADH4 in adjacent normal tissues (NT) and HCC tissues, The nuclei were stained with in blue. PLOD2 positive staining shown in the cytoplasm (Red). G6PD positive staining shown in the cytoplasm (Green). FTCD positive staining shown in the cytoplasm (Pink), ADH4 positive staining shown in the cytoplasm (Orange), and the nuclear counter stain is DAPI (Blue).

The potential applications of RCDRS in immunotherapy

Next, we investigated the predictive value of RCDRS in HCC patient's immunotherapy. The relative expression of key immune checkpoint: co-inhibitory checkpoints (IAP) (Figure 8A), immune co-stimulator checkpoints (ICP) (Figure 8B), and major histocompatibility complex (MHC) (Figure 8C) molecules showed that the expression levels were all higher in high-RCDRS groups and lower in low-RCDRS groups. These findings indicate that patients categorized in the low-RCDRS groups have a higher likelihood of experiencing favorable outcomes with immunotherapy. Additionally, the results obtained from the utilization of the tumor immune dysfunction and rejection (TIDE) tool[22] provide strong support for the proposition that patients in the low-RCDRS groups could potentially experience favorable outcomes with immunotherapy (Figure 8D). The analysis of IPS revealed that the low-RCDRS groups displayed higher scores, whereas the high-risk group exhibited lower scores, as depicted in Figure 8E. This finding provides additional confirmation for our previous hypothesis. Moreover, the correlation analysis between RCDRS and immunotherapy-related pathways (Figure 8F) further supports a significant association between RCDRS and these pathways. More importantly, the predictor efficiency of the RCDRS in urothelial carcinoma (IMvigor210 cohort)[23] and melanoma (Liu et al. cohort)[24] with immunotherapy was validated, and the Kaplan–Meir analysis showed statistically significant difference between the two cohort which is the patients with low-RCDRS had better overall survival (Figures 8G and 8H). The non-immunotherapy cohorts Kaplan–Meir results also further showed a trend toward higher ICIs efficacy in patients with low-RCDRS (Figures 8I and 8J). In summary, all consistent results demonstrated that RCDRS might be a potential signature for predicting the response of chemotherapy and immunotherapy.

DISCUSSION

Although many guidelines (NCCN, ESAL, ESMO and CSCO, etc.) has been clearly suggested ICIs-based immunotherapy as the first-line treatment which could improve the survival rate in variety of cancer types, the tumor response rate of advanced HCC is still very limited (14%–23%).[25–28] The limits of current immunotherapies were closely related to the TMB, TIME and epigenetic modification.[29] Several studies have revealed non-apoptotic RCD can affect tumor progression and its responsiveness to therapy by modulating immune cells and their functional manifestations,[12] but none of comprehensive analysis about the association between non-apoptotic RCD and HCC immune infiltration. Therefore, it is of great significance to establish a more effective scoring panel which could provide guidance for predicting prognosis and ICIs efficacy in HCC.

In recent years, molecular characterization based on genomics and bioinformatics has played a pivotal role in diagnosis, precision therapeutic and prognosis monitoring in various types of malignancy.[30,31] Previous studies have identified great significance HCC subtypes
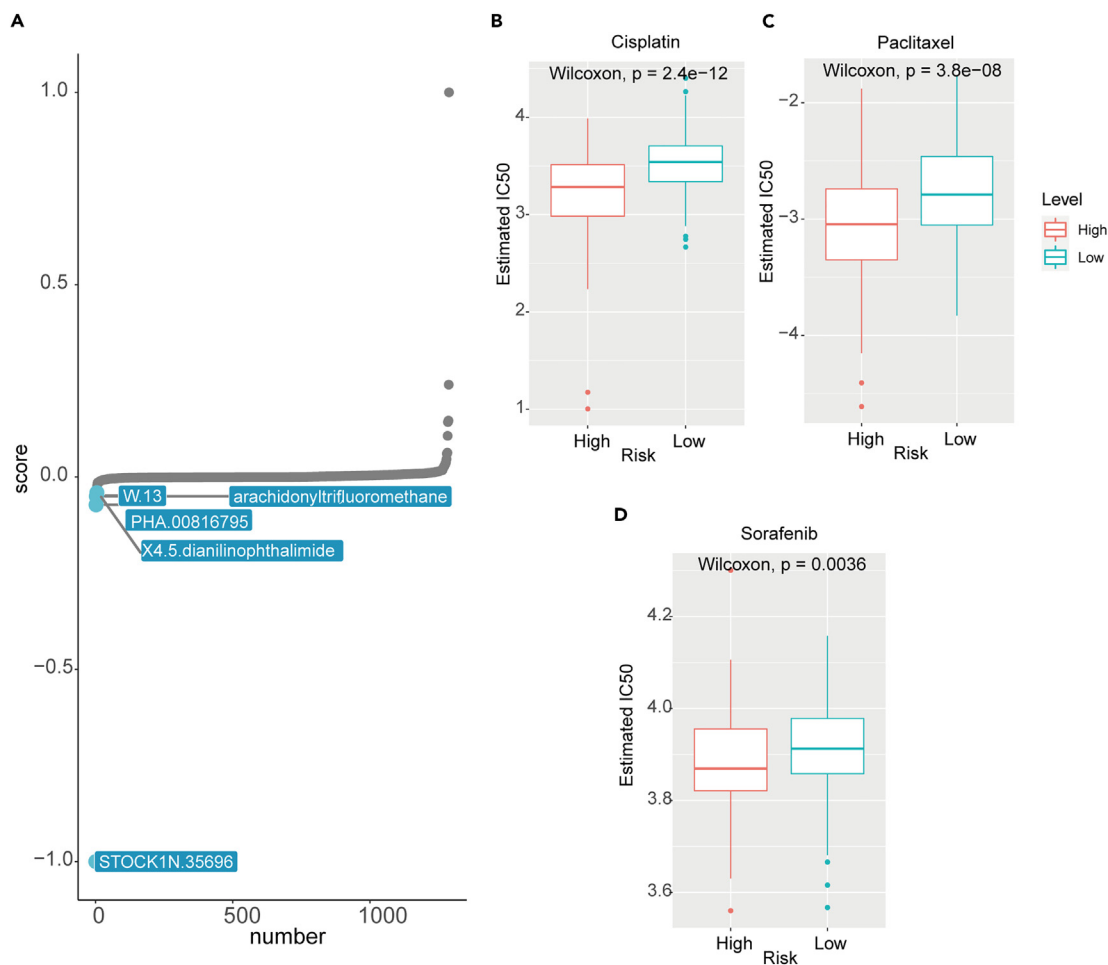
Figure 7. The predictive value of RCDRS in chemotherapy drugs selection and responsiveness in two risk groups

(A) Top5 small-molecule compounds with RCDRS.

(B) The estimated IC50 of cisplatin with high- and low-RCDRS groups.

(C) The estimated IC50 of paclitaxel with high- and low-RCDRS groups.

(D) The estimated IC50 of sorafenib with high- and low-RCDRS groups. Data are represented as mean (SD).

through multiple modalities and revealed the complex interplay of the tumor ecosystem during HCC development and progression.[32–34] For example, Chen et al.[35] had constructed an effective classification strategy to predict HCC progression and immunotherapy response by revealing metabolites and protein interactions (MPIs) in HCC development. However, there is still a lack of a systematic and comprehensive potential efficacy marker to indicate the prognosis and ICIs efficacy in HCC patients. Here, based on the critical roles of non-apoptotic RCD in determining tumor progression, TIME infiltration, and ICIs responsiveness, a total of 507 non-apoptotic RCD genes and 368 TCGA HCC samples were assigned into two optimal clusters, with better prognosis in cluster 1 groups than in cluster 2 groups. These results suggested that non-apoptotic RCD genes could mediate the classification of HCC subtypes. Meanwhile, we further systematically analyzed the significant differences in biological functions, TIME characteristics, mutation patterns, and epigenetic alternations between the two clusters, and established a reliable RCDSR panel. Moreover, the accuracy and predictive value of the panel in the prognosis and precision therapeutic of patients was validated by tissue samples and two cohorts, respectively.

Now, there are two important strategies to target immunosuppression in HCC, one is targeting VEGF signaling and another is targeting TGF-β signaling, whereas more than half of the HCC patients are still not responded to the combination targeted therapy.[8] Several potential targeted signaling pathways have been proposed, such as Wnt/β-catenin activation involved in immune exclusion in HCC and considered as a potential biomarker of immunotherapy resistance, but still need prospective confirmation.[36] In this study, we used GSVA to find significant differences in TIME and biological characteristics of the non-apoptotic RCD clusters, it manifested that mitotic spindle was activated in the cluster1 group, while KRAS signaling was downregulated in the cluster2 group. These meanings that mitotic spindle[37] and KRAS signaling[38] might be a critical pathway in targeting non-apoptotic RCD in HCC. Given the importance of immune cell infiltration for tumor immunotarget therapy, we focus on the immune cells in TIME which might affect tumors' behaviors and their responses to therapy. Besides, immune cell
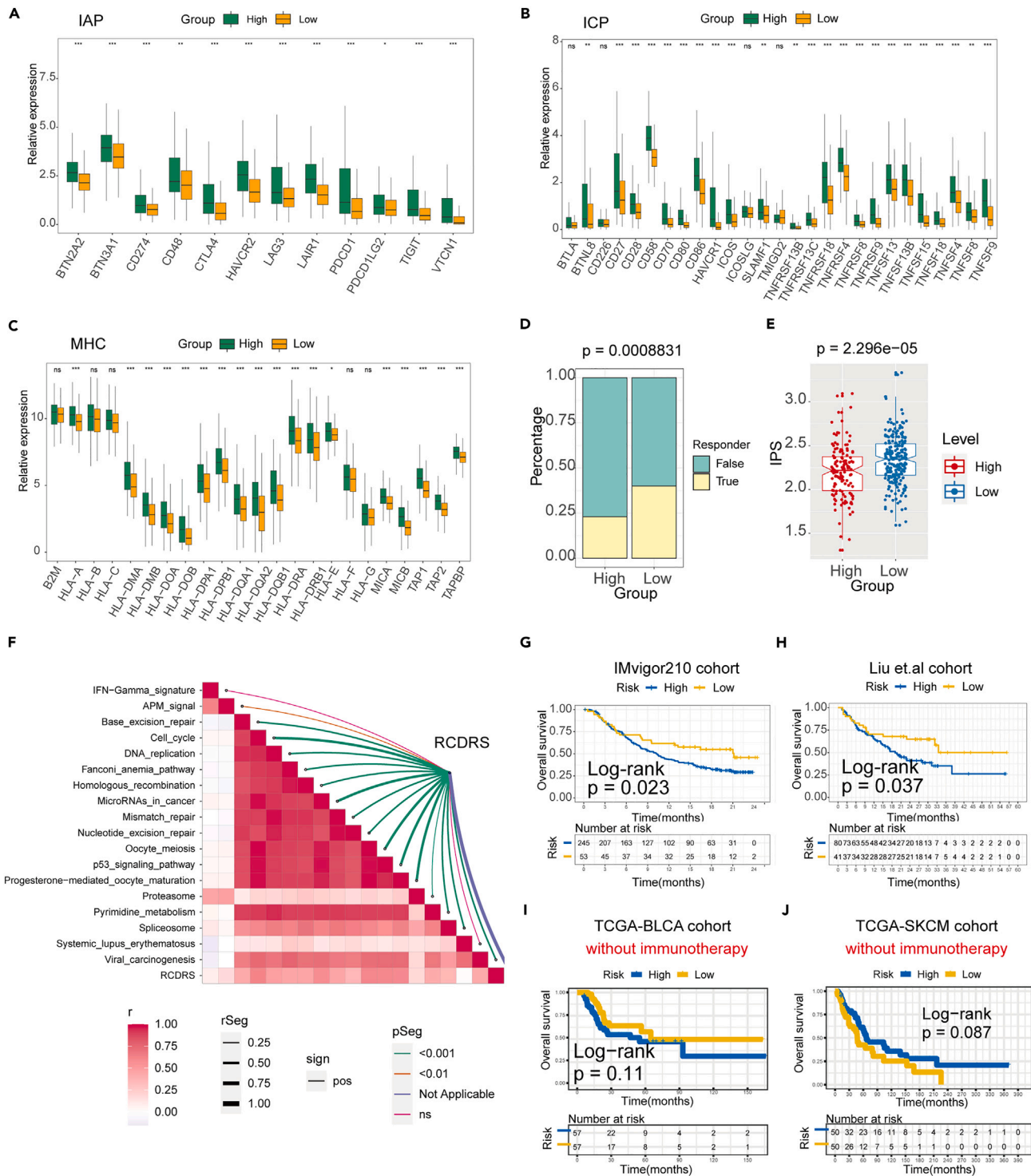
Figure 8. Prediction of response to immunotherapy by RCDRS

(A–C) The gene expression level of the gene set (IAP, ICP, and MHC) were showed in high- and low-RCDRS groups.

(D) The proportion of immunotherapy response rates were analyzed between the two groups by TIDE.

(E) The boxplot showed the IPS between high- and low-groups.

(F) The correlation of RCDRS and immunotherapy-related pathway.

(G) Kaplan-Meier analysis of the high- and low-RCDRS subgroups in the IMvigor210 cohort.

subtype analysis also revealed significant differences between the two clusters, including a variety of T cells, B cells, and DC cells. In summary, these results demonstrated that non-apoptotic RCD could regulate the TIME characteristics and immune cells infiltrating in HCC. Unfortunately, our understanding of the other cellular and non-cellular components in TIME and their mechanisms of action is insufficient.

HCC is an extremely heterogeneous tumor both in pathologically and molecular level, and this phenotype is closely related to gene mutation and transcriptome classification, which also affects the biological behavior and clinical characteristics of cancer cells.[39] Therefore, further exploration of gene mutation and transcriptome analysis based on non-apoptotic RCD will be helpful for immunotherapy and prognostic monitoring of HCC. Previous research has shown that the most common gene mutations in HCC were TP53,[38] CTNNB1[39] and ARID1A.[40] In our study, we determined four SMG including TP53, ALB, OBSCN, and SPTA1 in LIHC samples among non-apoptotic RCD subtypes. TP53 mutation is mainly identified in multiple poorly differentiated cancers and its inactivation in HCC was noticeably linked with clinical correlates, pathological and non-apoptotic RCD.[41,42] The mutational signatures extracted from COSMIC database showed that cluster1 groups were mainly related to DNA damage and repair, while cluster2 might associated with factors such as smoking. Moreover, we further found 1q21.3, 5q35.3, and 6p25.2 amplifications, 1p36.11, 4q21.3, 4q24 deletions, and more copy number gain and loss in cluster1 groups besides 6p21 (VEGFA) and 11q13 (FGF19/CNND1) amplifications and 9 (CDKN2A) homozygous deletions had previously reported in HCC.[43] In addition, we also found that non-apoptotic RCD could not only directly promote methylation modification in HCC cells, but also promote the expression of methylation-modified genes. This further demonstrated that the role of non-apoptotic RCD in epigenetic alterations in HCC progression could not be ignored.

There are many factors which impact on the overall survival of HCC. In our study, we found multiple differences between the two RCD subtypes. The prognosis of the cluster1 subtype was poorer compared to the cluster2 subtype. Meanwhile, we found higher mutation levels of TP53 in the cluster1 subtype (Figure 3A). The mutation patterns also indicated that the cluster1 subtype may have a deficiency in DNA damage and repair. In addition, cluster1 patients also had higher CNV, both at the arm and focal levels (Figure 4B). The results of the TIME showed that there were differences in the levels of multiple immune cell types (T cells CD4 memory resting, T cells CD4 memory activated, T cells CD4 naive) between the two subtypes (Figure 2B). Overall, the prognostic differences between the two subtypes may be explained by the above multiple-omics.

Through above studies, we can see clearly that non-apoptotic RCD had significant value in HCC classification. However, few tumors prognostic models have focused on predicting HCC prognosis and ICIs efficacy based on non-apoptotic RCD-associated markers. Therefore, it is essential to construct a non-apoptotic RCD-based panel RCDRS as an independent prognostic biomarker for predicting HCC prognosis and ICIs efficacy. Here, we finally constructed an RCDRS which obtained four mRNAs by multiple regression analysis. PLOD2 and G6PD, the non-apoptosis RCD (necroptosis, ferroptosis, autophagy)-related gene signature which can as an effective prognostic marker associated with prognosis, immune landscape, drug sensitivity, and HCC tumorigenesis.[44–47] And FTCD and ADH4(inflammation-associated ferroptosis signature)[48] as a tumor suppressor gene, over-expression of FTCD and ADH4 significantly inhibited the proliferation and promoted apoptosis in HCC.[49–51] Most importantly, the expression and cellular localization of these four genes in HCC and adjacent normal tissues were verified in detail from the perspective of gene expression and protein translation by multiple assays. All the results finally proved that non-apoptotic RCD plays a critical role in HCC carcinogenesis. This further indicated that our RCDRS panel based on the four key non-apoptotic RCD genes was reliable and effectivity.

Meanwhile, we used TCGA-LIHC patients for corresponding validation, and the results showed that high-RCDRS group had a markedly lower survival probability than that the low-RCDRS group, and the calibration plots for the 3- and 5-year OS predicted well. Although the 3- and 5-year OS were not significantly different from those of many other reported models.[52–54] The main advantage of our study is that it combined TME characteristics and biological features, mutation patterns, genetic and methylation changes non-apoptotic RCD for HCC patients. Therefore, this RCDRS panel still might be a promising tool for clinicians to comprehensively assess the patient's prognosis and chemotherapy and ICIs efficacy in the future.

To further understand the clinical applicability and practicability of RCDRS, the relationship between RCDRS and clinical therapy was explored by XSum algorithm and TIDE tool. The results showed that high-RCDRS group patients had drug benefits in STOCK1N.35696 and had the lower estimated IC50 in anti-tumor drugs (cisplatin, paclitaxel, and sorafenib) which can induce non-apoptotic RCD.[55–57] These findings provided a promising therapy opportunity for HCC patients, but further clinical validations are needed to verify. In addition, the responsiveness analysis of immune checkpoint blockade also showed a trend toward higher ICIs efficacy in patients with low-RCDRS. Amazingly, when we validated the predictor efficiency of RCDRS in two immunotherapy cohorts, it also showed that low-RCDRS patients had better OS. This indicated that our RCDRS might be used as an effective predictor of prognosis and ICIs efficacy not only in patients with HCC, but also in patients with other cancers.

In conclusion, our preliminary analysis found that non-apoptotic RCD played a key role in HCC progression and prognosis. Based on this clue, the significant differences in biological functions, TIME characteristics, mutation patterns, genetic and methylation alternations between the two clusters were systematically analyzed. The RCDRS scoring panel for risk assessment of HCC patients was established, and the key reliability was verified by HCC tissues. Moreover, we found that the scoring panel could screen better responsive chemotherapy and

immunotherapy drugs for cancer patients and validated the scoring panel in two immunotherapy cohorts. In short, we established a panel for predicting the prognosis and potential therapeutic drug selection in HCC patients, which may improve the clinical demand of HCC to a certain extent.

Limitations of the study

However, our study still presents several limitations. First, these conclusions are mainly based on bioinformatics mining of public databases, and their reliability still needs to be verified by more clinical HCC samples. Second, with the core research of non-apoptotic RCD, this study has discovered many valuable results in HCC progression, such as various immune cell infiltration and epigenetic alternations. How they interact with each other, and then affect the progression, therapy, and prognosis of HCC, which were not well elucidated in this study. Finally, this study was only a preliminary finding of the importance of non-apoptotic RCD in HCC and its feasibility for the classification, However, the underlying mechanisms of these RCDRS in HCC progression and immune escape have not been thoroughly studied.

STAR★METHODS

Detailed methods are provided in the online version of this paper and include the following:

- KEY RESOURCES TABLE
- RESOURCE AVAILABILITY
  - Lead contact
  - Materials availability
  - Data and code availability
- EXPERIMENTAL MODEL AND STUDY PARTICIPANT DETAILS
  - Ethics statement
- METHOD DETAILS
  - Publicly data collection and preprocessing
  - Consensus cluster of non-apoptotic RCD-related genes
  - TIME infiltration and immunophenoscore (IPS) analysis
  - Geneset variation analysis (GSVA)
  - Genomic mutation, methylation diver gene and copy number variation (CNV) analysis
  - Generation of non-apoptotic RCD-related signature in HCC patients
  - Prediction of chemotherapeutic responses and potential small molecule drugs
  - HCC patients tissue samples collection
  - Quantitative real-time PCR (qRT-PCR) analysis
  - Immunohistochemistry staining
  - Multiplexed immunofluorescence staining
- QUANTIFICATION AND STATISTICAL ANALYSIS
  - Additional resources

SUPPLEMENTAL INFORMATION

Supplemental information can be found online at https://doi.org/10.1016/j.isci.2024.109901.

AUTHOR CONTRIBUTIONS

S.L., Y.X., X.H., and H.C. contributed equally. F.W., J.W., and C.Y. contributed to the study concept and design of this study. S.L., X.H., and Y.X. contributed to the acquisition, analysis, interpretation of data. X.X., H.C., F.L., and Y.R. contributed to sample collection and performed the pathological examination. X.H. and W.J. contributed to draft of the manuscript. F.W., C.L., and C.Y. provided final review and revision of the manuscript. All authors gave final approval to this manuscript for publication.

DECLARATION OF INTERESTS

The authors declare no competing interests.

REFERENCES

1. Sung, H., Ferlay, J., Siegel, R.L., Laversanne, M., Soerjomataram, I., Jemal, A., and Bray, F. (2021). Global Cancer Statistics 2020: GLOBOCAN Estimates of Incidence and Mortality Worldwide for 36 Cancers in 185 Countries. CA. Cancer J. Clin. 71, 209–249. https://doi.org/10.3322/caac.21660.

2. Llovet, J.M., Castet, F., Heikenwalder, M., Maini, M.K., Mazzaferro, V., Pinato, D.J., Pikarsky, E., Zhu, A.X., and Finn, R.S. (2022). Immunotherapies for hepatocellular carcinoma. Nat. Rev. Clin. Oncol. 19, 151–172. https://doi.org/10.1038/s41571-021-00573-2.

3. Kelley, R.K., Sangro, B., Harris, W., Ikeda, M., Okusaka, T., Kang, Y.K., Qin, S., Tai, D.W.M., Lim, H.Y., Yau, T., et al. (2021). Safety, Efficacy, and Pharmacodynamics of Tremelimumab Plus Durvalumab for Patients With Unresectable Hepatocellular Carcinoma: Randomized Expansion of a Phase I/II Study. J. Clin. Oncol. 39, 2991–3001. https://doi.org/10.1200/jco.20.03555.

4. Finn, R.S., Ikeda, M., Zhu, A.X., Sung, M.W., Baron, A.D., Kudo, M., Okusaka, T., Kobayashi, M., Kumada, H., Kaneko, S., et al. (2020). Phase Ib Study of Lenvatinib Plus Pembrolizumab in Patients With Unresectable Hepatocellular Carcinoma. J. Clin. Oncol. 38, 2960–2970. https://doi.org/10.1200/JCO.20.00808.

5. Thorsson, V., Gibbs, D.L., Brown, S.D., Wolf, D., Bortone, D.S., Ou Yang, T.H., Porta-Pardo, E., Gao, G.F., Plaisier, C.L., Eddy, J.A., et al. (2018). The Immune Landscape of Cancer. Immunity 48, 812–830.e14. https://doi.org/10.1016/j.immuni.2018.03.023.

6. Finn, R.S., Qin, S., Ikeda, M., Galle, P.R., Ducreux, M., Kim, T.Y., Kudo, M., Breder, V., Merle, P., Kaseb, A.O., et al. (2020). Atezolizumab plus Bevacizumab in Unresectable Hepatocellular Carcinoma. N. Engl. J. Med. 382, 1894–1905. https://doi.org/10.1056/NEJMoa1915745.

7. Rebouissou, S., and Nault, J.C. (2020). Advances in molecular classification and precision oncology in hepatocellular carcinoma. J. Hepatol. 72, 215–229. https://doi.org/10.1016/j.jhep.2019.08.017.

8. Pinter, M., Jain, R.K., and Duda, D.G. (2021). The Current Landscape of Immune Checkpoint Blockade in Hepatocellular Carcinoma: A Review. JAMA Oncol. 7, 113–123. https://doi.org/10.1001/jamaoncol.2020.3381.

9. El-Khoueiry, A.B., Sangro, B., Yau, T., Crocenzi, T.S., Kudo, M., Hsu, C., Kim, T.Y., Choo, S.P., Trojan, J., Welling, T.H., Rd, et al. (2017). Nivolumab in patients with advanced hepatocellular carcinoma (CheckMate 040): an open-label, non-comparative, phase 1/2 dose escalation and expansion trial. Lancet 389, 2492–2502. https://doi.org/10.1016/S0140-6736(17)31046-2.

10. Sangro, B., Melero, I., Wadhawan, S., Finn, R.S., Abou-Alfa, G.K., Cheng, A.L., Yau, T., Furuse, J., Park, J.W., Boyd, Z., et al. (2020). Association of inflammatory biomarkers with clinical outcomes in nivolumab-treated patients with advanced hepatocellular carcinoma. J. Hepatol. 73, 1460–1469. https://doi.org/10.1016/j.jhep.2020.07.026.

11. Haber, P.K., Torres-Martin, M., Dufour, J.-F., Verslype, C., Marquardt, J., Galle, P.R., Vogel, A., Meyer, T., Labgaa, I., Roberts, L.R., et al. (2021). Molecular markers of response to anti-PD1 therapy in advanced hepatocellular carcinoma. J. Clin. Oncol. 39, 4100. https://doi.org/10.1200/JCO.2021.39.15_suppl.4100.

12. Gao, W., Wang, X., Zhou, Y., Wang, X., and Yu, Y. (2022). Autophagy, ferroptosis, pyroptosis, and necroptosis in tumor immunotherapy. Signal Transduct. Target. Ther. 7, 196. https://doi.org/10.1038/s41392-022-01046-3.

13. Wang, Q., Wang, Y., Ding, J., Wang, C., Zhou, X., Gao, W., Huang, H., Shao, F., and Liu, Z. (2020). A bioorthogonal system reveals antitumour immune function of pyroptosis. Nature 579, 421–426. https://doi.org/10.1038/s41586-020-2079-1.

14. Rothlin, C.V., Hille, T.D., and Ghosh, S. (2021). Determining the effector response to cell death. Nat. Rev. Immunol. 21, 292–304. https://doi.org/10.1038/s41577-020-00456-0.

15. Tsvetkov, P., Coy, S., Petrova, B., Dreishpoon, M., Verma, A., Abdusamad, M., Rossen, J., Joesch-Cohen, L., Humeidi, R., Spangler, R.D., et al. (2022). Copper induces cell death by targeting lipoylated TCA cycle proteins. Science 375, 1254–1261. https://doi.org/10.1126/science.abf0529.

16. Seehawer, M., Heinzmann, F., D'Artista, L., Harbig, J., Roux, P.F., Hoenicke, L., Dang, H., Klotz, S., Robinson, L., Doré, G., et al. (2018). Necroptosis microenvironment directs lineage commitment in liver cancer. Nature 562, 69–75. https://doi.org/10.1038/s41586-018-0519-y.

17. Xu, W.P., Liu, J.P., Feng, J.F., Zhu, C.P., Yang, Y., Zhou, W.P., Ding, J., Huang, C.K., Cui, Y.L., Ding, C.H., et al. (2020). miR-541 potentiates the response of human hepatocellular carcinoma to sorafenib treatment by inhibiting autophagy. Gut 69, 1309–1321. https://doi.org/10.1136/gutjnl-2019-318830.

18. Hage, C., Hoves, S., Strauss, L., Bissinger, S., Prinz, Y., Pöschinger, T., Kiessling, F., and Ries, C.H. (2019). Sorafenib Induces Pyroptosis in Macrophages and Triggers Natural Killer Cell-Mediated Cytotoxicity Against Hepatocellular Carcinoma. Hepatology 70, 1280–1297. https://doi.org/10.1002/hep.30666.

19. Gao, R., Kalathur, R.K.R., Coto-Llerena, M., Ercan, C., Buechel, D., Shuang, S., Piscuoglio, S., Dill, M.T., Camargo, F.D., Christofori, G., and Tang, F. (2021). YAP/TAZ and ATF4 drive resistance to Sorafenib in hepatocellular carcinoma by preventing ferroptosis. EMBO Mol. Med. 13, e14351. https://doi.org/10.15252/emmm.202114351.

20. Zhang, Z., Zeng, X., Wu, Y., Liu, Y., Zhang, X., and Song, Z. (2022). Cuproptosis-Related Risk Score Predicts Prognosis and Characterizes the Tumor Microenvironment in Hepatocellular Carcinoma. Front. Immunol. 13, 925618. https://doi.org/10.3389/fimmu.2022.925618.

21. Feinberg, A.P., and Levchenko, A. (2023). Epigenetics as a mediator of plasticity in cancer. Science 379, eaaw3835. https://doi.org/10.1126/science.aaw3835.

22. Jiang, P., Gu, S., Pan, D., Fu, J., Sahu, A., Hu, X., Li, Z., Traugh, N., Bu, X., Li, B., et al. (2018). Signatures of T cell dysfunction and exclusion predict cancer immunotherapy response. Nat. Med. 24, 1550–1558. https://doi.org/10.1038/s41591-018-0136-1.

23. Mariathasan, S., Turley, S.J., Nickles, D., Castiglioni, A., Yuen, K., Wang, Y., Kadel, E.E., III, Koeppen, H., Astarita, J.L., Cubas, R., et al. (2018). TGFbeta attenuates tumour response to PD-L1 blockade by contributing to exclusion of T cells. Nature 554, 544–548. https://doi.org/10.1038/nature25501.

24. Liu, D., Schilling, B., Liu, D., Sucker, A., Livingstone, E., Jerby-Arnon, L., Zimmer, L., Gutzmer, R., Satzger, I., Loquai, C., et al. (2019). Integrative molecular and clinical modeling of clinical outcomes to PD1 blockade in patients with metastatic melanoma. Nat. Med. 25, 1916–1927. https://doi.org/10.1038/s41591-019-0654-5.

25. Benson, A.B., D'Angelica, M.I., Abbott, D.E., Anaya, D.A., Anders, R., Are, C., Bachini, M., Borad, M., Brown, D., Burgoyne, A., et al. (2021). Hepatobiliary Cancers, Version 2.2021, NCCN Clinical Practice Guidelines in Oncology. J. Natl. Compr. Canc. Netw. 19, 541–565. https://doi.org/10.6004/jnccn.2021.0022.

26. European Association for the Study of the Liver Electronic address easloffice@easlofficeeu European Association for the Study of the, L (2018). EASL Clinical Practice Guidelines: Management of hepatocellular carcinoma. J. Hepatol. 69, 182–236. https://doi.org/10.1016/j.jhep.2018.03.019.

27. Vogel, A., and Martinelli, E.; ESMO Guidelines Committee Electronic address clinicalguidelines@esmoorg (2021). Updated treatment recommendations for hepatocellular carcinoma (HCC) from the ESMO Clinical Practice Guidelines. Ann. Oncol. 32, 801–805. https://doi.org/10.1016/j.annonc.2021.02.014.

28. Xie, D.Y., Ren, Z.G., Zhou, J., Fan, J., and Gao, Q. (2020). 2019 Chinese clinical guidelines for the management of hepatocellular carcinoma: updates and insights. Hepatobiliary Surg. Nutr. 9, 452–463. https://doi.org/10.21037/hbsn-20-480.

29. Zhong, C., Li, Y., Yang, J., Jin, S., Chen, G., Li, D., Fan, X., and Lin, H. (2021). Immunotherapy for Hepatocellular Carcinoma: Current Limits and Prospects. Front. Oncol. 11, 589680. https://doi.org/10.3389/fonc.2021.589680.

30. Dai, Y., Qiang, W., Lin, K., Gui, Y., Lan, X., and Wang, D. (2021). An immune-related gene signature for predicting survival and immunotherapy efficacy in hepatocellular carcinoma. Cancer Immunol. Immunother. 70, 967–979. https://doi.org/10.1007/s00262-020-02743-0.

31. Canzoneri, R., Lacunza, E., and Abba, M.C. (2019). Genomics and bioinformatics as pillars of precision medicine in oncology. Medicina 79, 587–592.

32. Cancer Genome Atlas Research Network Electronic address wheeler@bcmedu Cancer

Genome Atlas Research Network (2017). Comprehensive and Integrative Genomic Characterization of Hepatocellular Carcinoma. Cell 169, 1327–1341.e23. https://doi.org/10.1016/j.cell.2017.05.046.

33. Gu, X., Guan, J., Xu, J., Zheng, Q., Chen, C., Yang, Q., Huang, C., Wang, G., Zhou, H., Chen, Z., and Zhu, H. (2021). Model based on five tumour immune microenvironment-related genes for predicting hepatocellular carcinoma immunotherapy outcomes. J. Transl. Med. 19, 26. https://doi.org/10.1186/s12967-020-02691-4.

34. Yang, C., Huang, X., Liu, Z., Qin, W., and Wang, C. (2020). Metabolism-associated molecular classification of hepatocellular carcinoma. Mol. Oncol. 14, 896–913. https://doi.org/10.1002/1878-0261.12639.

35. Chen, D., Zhang, Y., Wang, W., Chen, H., Ling, T., Yang, R., Wang, Y., Duan, C., Liu, Y., Guo, X., et al. (2021). Identification and Characterization of Robust Hepatocellular Carcinoma Prognostic Subtypes Based on an Integrative Metabolite-Protein Interaction Network. Adv. Sci. 8, e2100311. https://doi.org/10.1002/advs.202100311.

36. Ruiz de Galarreta, M., Bresnahan, E., Molina-Sánchez, P., Lindblad, K.E., Maier, B., Sia, D., Puigvehi, M., Miguela, V., Casanova-Acebes, M., Dhainaut, M., et al. (2019). beta-Catenin Activation Promotes Immune Escape and Resistance to Anti-PD-1 Therapy in Hepatocellular Carcinoma. Cancer Discov. 9, 1124–1141. https://doi.org/10.1158/2159-8290.CD-19-0074.

37. Liu, X., Li, Y., Meng, L., Liu, X.Y., Peng, A., Chen, Y., Liu, C., Chen, H., Sun, S., Miao, X., et al. (2018). Reducing protein regulator of cytokinesis 1 as a prospective therapy for hepatocellular carcinoma. Cell Death Dis. 9, 534. https://doi.org/10.1038/s41419-018-0555-4.

38. Hill, M.A., Alexander, W.B., Guo, B., Kato, Y., Patra, K., O'Dell, M.R., McCall, M.N., Whitney-Miller, C.L., Bardeesy, N., and Hezel, A.F. (2018). Kras and Tp53 Mutations Cause Cholangiocyte- and Hepatocyte-Derived Cholangiocarcinoma. Cancer Res. 78, 4445–4451. https://doi.org/10.1158/0008-5472.CAN-17-1123.

39. Calderaro, J., Couchy, G., Imbeaud, S., Amaddeo, G., Letouzé, E., Blanc, J.F., Laurent, C., Hajji, Y., Azoulay, D., Bioulac-Sage, P., et al. (2017). Histological subtypes of hepatocellular carcinoma are related to gene mutations and molecular tumour classification. J. Hepatol. 67, 727–738. https://doi.org/10.1016/j.jhep.2017.05.014.

40. Zhang, S., Zhou, Y.F., Cao, J., Burley, S.K., Wang, H.Y., and Zheng, X.F.S. (2021). mTORC1 Promotes ARID1A Degradation and Oncogenic Chromatin Remodeling in Hepatocellular Carcinoma. Cancer Res. 81, 5652–5665. https://doi.org/10.1158/0008-5472.CAN-21-0206.

41. Mirgayazova, R., Khadiullina, R., Chasov, V., Mingaleeva, R., Miftakhova, R., Rizvanov, A., and Bulatov, E. (2020). Therapeutic Editing of the TP53 Gene: Is CRISPR/Cas9 an Option? Genes 11, 704. https://doi.org/10.3390/genes11060704.

42. Yang, C., Huang, X., Li, Y., Chen, J., Lv, Y., and Dai, S. (2021). Prognosis and personalized treatment prediction in TP53-mutant hepatocellular carcinoma: an in silico strategy towards precision oncology. Brief. Bioinform. 22, bbaa164. https://doi.org/10.1093/bib/bbaa164.

43. Zucman-Rossi, J., Villanueva, A., Nault, J.C., and Llovet, J.M. (2015). Genetic Landscape and Biomarkers of Hepatocellular Carcinoma. Gastroenterology 149, 1226–1239.e4. https://doi.org/10.1053/j.gastro.2015.05.061.

44. Du, H., Pang, M., Hou, X., Yuan, S., and Sun, L. (2017). PLOD2 in cancer research. Biomed. Pharmacother. 90, 670–676. https://doi.org/10.1016/j.biopha.2017.04.023.

45. Li, G., Wang, X., and Liu, G. (2021). PLOD2 Is a Potent Prognostic Marker and Associates with Immune Infiltration in Cervical Cancer. BioMed Res. Int. 2021, 5512340. https://doi.org/10.1155/2021/5512340.

46. Lu, M., Lu, L., Dong, Q., Yu, G., Chen, J., Qin, L., Wang, L., Zhu, W., and Jia, H. (2018). Elevated G6PD expression contributes to migration and invasion of hepatocellular carcinoma cells by inducing epithelial-mesenchymal transition. Acta Biochim. Biophys. Sin. 50, 370–380. https://doi.org/10.1093/abbs/gmy009.

47. Cao, F., Luo, A., and Yang, C. (2021). G6PD inhibits ferroptosis in hepatocellular carcinoma by targeting cytochrome P450 oxidoreductase. Cell. Signal. 87, 110098. https://doi.org/10.1016/j.cellsig.2021.110098.

48. Ruan, W.Y., Zhang, L., Lei, S., Zeng, Z.R., Yang, Y.S., Cao, W.P., Hao, Q.Y., Lu, M., Tian, X.B., and Peng, P.L. (2023). An inflammation-associated ferroptosis signature optimizes the diagnosis, prognosis evaluation and immunotherapy options in hepatocellular carcinoma. J. Cell Mol. Med. 27, 1820–1835. https://doi.org/10.1111/jcmm.17780.

49. Chen, J., Yang, Y., Lin, B., Xu, Z., Yang, X., Ye, S., Xie, Z., Li, Y., Hong, J., Huang, Z., and Huang, W. (2022). Hollow mesoporous organosilica nanotheranostics incorporating formimidoyltransferase cyclodeaminase (FTCD) plasmids for magnetic resonance imaging and tetrahydrofolate metabolism fission on hepatocellular carcinoma. Int. J. Pharm. 612, 121281. https://doi.org/10.1016/j.ijpharm.2021.121281.

50. Xu, D., Wang, Y., Wu, J., Lin, S., Chen, Y., and Zheng, J. (2021). Identification and clinical validation of EMT-associated prognostic features based on hepatocellular carcinoma. Cancer Cell Int. 21, 621. https://doi.org/10.1186/s12935-021-02326-8.

51. Chowdhury, N.P., Moon, J., and Müller, V. (2021). Adh4, an alcohol dehydrogenase controls alcohol formation within bacterial microcompartments in the acetogenic bacterium Acetobacterium woodii. Environ. Microbiol. 23, 499–511. https://doi.org/10.1111/1462-2920.15340.

52. Liu, G.M., Zeng, H.D., Zhang, C.Y., and Xu, J.W. (2019). Identification of a six-gene signature predicting overall survival for hepatocellular carcinoma. Cancer Cell Int. 19, 138. https://doi.org/10.1186/s12935-019-0858-2.

53. Chen, Q., Li, F., Gao, Y., Xu, G., Liang, L., and Xu, J. (2020). Identification of Energy Metabolism Genes for the Prediction of Survival in Hepatocellular Carcinoma. Front. Oncol. 10, 1210. https://doi.org/10.3389/fonc.2020.01210.

54. Yan, Z., He, M., He, L., Wei, L., and Zhang, Y. (2021). Identification and Validation of a Novel Six-Gene Expression Signature for Predicting Hepatocellular Carcinoma Prognosis. Front. Immunol. 12, 723271. https://doi.org/10.3389/fimmu.2021.723271.

55. Deng, F., Zheng, X., Sharma, I., Dai, Y., Wang, Y., and Kanwar, Y.S. (2021). Regulated cell death in cisplatin-induced AKI: relevance of myo-inositol metabolism. Am. J. Physiol. Renal Physiol. 320, F578–F595. https://doi.org/10.1152/ajprenal.00016.2021.

56. Tang, M., Zhao, S., Liu, J.X., Liu, X., Guo, Y.X., Wang, G.Y., and Wang, X.L. (2022). Paclitaxel induces cognitive impairment via necroptosis, decreased synaptic plasticity and M1 polarisation of microglia. Pharm. Biol. 60, 1556–1565. https://doi.org/10.1080/13880209.2022.2108064.

57. Zheng, X., Liu, B., Liu, X., Li, P., Zhang, P., Ye, F., Zhao, T., Kuang, Y., Chen, W., Jin, X., and Li, Q. (2022). PERK Regulates the Sensitivity of Hepatocellular Carcinoma Cells to High-LET Carbon Ions via either Apoptosis or Ferroptosis. J. Cancer 13, 669–680. https://doi.org/10.7150/jca.61622.

58. Charoentong, P., Finotello, F., Angelova, M., Mayer, C., Efremova, M., Rieder, D., Hackl, H., and Trajanoski, Z. (2017). Pan-cancer Immunogenomic Analyses Reveal Genotype-Immunophenotype Relationships and Predictors of Response to Checkpoint Blockade. Cell Rep. 18, 248–262. https://doi.org/10.1016/j.celrep.2016.12.019.

59. Geeleher, P., Cox, N., and Huang, R.S. (2014). pRRophetic: an R package for prediction of clinical chemotherapeutic response from tumor gene expression levels. PLoS One 9, e107468. https://doi.org/10.1371/journal.pone.0107468.

60. Geeleher, P., Cox, N.J., and Huang, R.S. (2014). Clinical drug response can be predicted using baseline gene expression levels and in vitro drug sensitivity in cell lines. Genome Biol. 15, R47. https://doi.org/10.1186/gb-2014-15-3-r47.

61. Yang, C., Zhang, H., Chen, M., Wang, S., Qian, R., Zhang, L., Huang, X., Wang, J., Liu, Z., Qin, W., et al. (2022). A survey of optimal strategy for signature-based drug repositioning and an application to liver cancer. Elife 11, e71880. https://doi.org/10.7554/eLife.71880.

62. Marrero, J.A., Kulik, L.M., Sirlin, C.B., Zhu, A.X., Finn, R.S., Abecassis, M.M., Roberts, L.R., and Heimbach, J.K. (2018). Diagnosis, Staging, and Management of Hepatocellular Carcinoma: 2018 Practice Guidance by the American Association for the Study of Liver Diseases. Hepatology 68, 723–750. https://doi.org/10.1002/hep.29913.

63. Chen, Y., Zitello, E., Guo, R., and Deng, Y. (2021). The function of LncRNAs and their role in the prediction, diagnosis, and prognosis of lung cancer. Clin. Transl. Med. 11, e367. https://doi.org/10.1002/ctm2.367.

64. Du, S., Qian, J., Tan, S., Li, W., Liu, P., Zhao, J., Zeng, Y., Xu, L., Wang, Z., and Cai, J. (2022). Tumor cell-derived exosomes deliver TIE2 protein to macrophages to promote angiogenesis in cervical cancer. Cancer Lett. 529, 168–179. https://doi.org/10.1016/j.canlet.2022.01.005.

STAR★METHODS

KEY RESOURCES TABLE

REAGENT or RESOURCE	SOURCE	IDENTIFIER
Antibodies		
anti-PLOD2 antibody	Proteintech	Cat# 21214-1-AP; RRID: AB_10733347
anti-G6PD antibody	Proteintech	Cat# 25413-1-AP; RRID: AB_2880066
anti-FTCD antibody	Proteintech	Cat# 21959-1-AP; RRID: AB_11182396
anti-ADH4 antibody	Proteintech	Cat# 16474-1-AP; RRID: AB_2223855
Biological samples		
Wuhan (20 HCC tumor tissues and matched adjacent normal tissues)	Zhongnan Hospital of Wuhan University	N/A
Chemicals, peptides, and recombinant proteins		
4% PFA	Biosharp	BL539A
Trizol reagent	Thermo Fisher Scientific	15596018CN
Critical commercial assays		
HiFiScript gDNA Removal RT MasterMix kit	CWBIO	CW2020M
MagicSYBR Mixture kits	CWBIO	CW3008M
Deposited data		
RT-qPCR data	This paper	Shared upon request by the Lead Contact
Somatic mutation information	TCGA	https://portal.gdc.cancer.gov/
TCGA-LIHC RNA-seq	TCGA	https://portal.gdc.cancer.gov/
TCGA-LIHC clinical data	UCSC Xena	https://xenabrowser.net/datapages/
GSE116174	GEO	https://www.ncbi.nlm.nih.gov/geo
Hallmark gene sets	Molecular Signaling Database (MSigDB)	https://www.gsea-msigdb.org/gsea/msigdb
Signaling pathways	FerrDb	http://www.zhounan.org/ferrdb/current/
Signaling pathways	Human Autophagy Database (HADb)	http://www.autophagy.lu/index.html
Mutational Signatures	Catalog of Somatic Mutations in Cancer	https://cancer.sanger.ac.uk/signatures/signatures_v2/
Oligonucleotides		
Primer for qRT-PCR assay	Sangon Biotech	Table S3
Software and algorithms		
R (4.1.1)	R Core Team	https://www.r-project.org/
ssGSEA	'GSEABase' R package	http://www.bioconductor.org
Chemotherapeutic response prediction	'pRRophetic' R package	https://github.com/
Consensus clustering analysis	ConsensusClusterPlus package	https://bioconductor.org/
GSVA	'GSVA' R package	https://bioconductor.org/
Somatic mutation gene analysis	'maftools' R package	https://bioconductor.org/
Differential methylation-driven genes identification	'MethylMix' R package	https://bioconductor.org
Draw waterfall plot and heatmap	'Complex HeatMap' R package	https://bioconductor.org
Matching method for drug retrieval	eXtreme Sum algorithm	https://github.com/
Cut-off value	'survminer' R package	https://www.rdocumentation.org/

RESOURCE AVAILABILITY

Lead contact

Further information and requests for resources and materials should be directed to and will be fulfilled by the lead contact, Fu-Bing Wang (wfb20042002@sina.com).

Materials availability

This study did not generate new unique reagents.

Data and code availability

- Datasets analyzed during the current study are available from open-access databases. Accession numbers for these databases are listed in the key resources table.
- Any additional information required to reanalyze the data reported in this paper is available from the lead contact upon request.
- No custom codes were used in the study.

EXPERIMENTAL MODEL AND STUDY PARTICIPANT DETAILS

The samples were all from HCC tissues with precise histological and pathological diagnoses. All cases in this study were anonymous and processed according to legal requirements and medical standards, approved by the Research Ethics Committees of Zhongnan Hospital (Ethical Approval number: 2023013). Informed consent was obtained from all patients for being included in the study. The clinical information of all HCC patients was summarized in Table S4.

Ethics statement

The human tissue sample used in this study were approved by the Research Ethics Committees of Zhongnan Hospital (Ethical Approval number: 2023013) and in accordance with the Helsinki Declaration of 1975, as revised in 2013. Informed consent was obtained from all patients for being included in the study.

METHOD DETAILS

Publicly data collection and preprocessing

The TCGA and GEO databases were utilized to gather publicly available gene expression data and associated clinical information for liver cancer. Here, we excluded patients with no survival information before analysis. The R software was employed to extract the RNA-seq fragments per kilobase of per million (FPKM) values and clinical data for the TCGA-Liver Hepatocellular Carcinoma (TCGA-LIHC: https://portal.gdc.cancer.gov/projects/TCGA-LIHC) cohort. Afterward, the FPKM values were transformed into transcripts per kilobase million (TPM) values. The batch effects were corrected by ComBat method and verified by principal component analysis (PCA). The initial step involved downloading the raw "CEL" files of the GEO microarray data. Subsequently, a robust multiarray averaging method was applied for proper normalization purposes. In total, we obtained TCGA-LIHC (N = 368) and GEO cohort: GSE116174 (N = 64) datasets as the eligible liver cancer cohorts for subsequent analysis. The workflow is shown in Figure S1 and the baseline characteristics of TCGA-LIHC cohort is summarized in Table S1.

Consensus cluster of non-apoptotic RCD-related genes

We extracted 507 non-apoptotic RCD genes from published literature,[15] FerrDb database: http://www.zhounan.org/ferrdb/current/, Human Autophagy Database (HADb: http://www.autophagy.lu/index.html), and MSigDB database: https://www.gsea-msigdb.org/gsea/msigdb/index.jsp (M24370 and M24779). The ConsensusClusterPlus package was employed to perform a consensus clustering analysis in order to identify unique transcriptional regulation patterns associated with non-apoptotic regulated cell death (RCD). To ensure reliability, this step was repeated up to 100 times.

TIME infiltration and immunophenoscore (IPS) analysis

Single sample gene set enrichment analysis (ssGSEA) was utilized to assess the relative infiltration levels of 25 various immune cell types in HCC patients. The enrichment scores represented the relative infiltrating abundance of each immune cells. The IPS was created based on immune-related genes as described previously.[58] Higher IPS represents better ICIs efficacy.

Geneset variation analysis (GSVA)

The "Hallmark gene sets" obtained from MSigDB were utilized for GSVA enrichment analysis performed with the "GSVA" R package. The resultant GSVA scores reflect the differential biological pathways of gene sets in each sample across various non-apoptotic regulated cell death (RCD) groups.

Genomic mutation, methylation diver gene and copy number variation (CNV) analysis

The significantly mutated genes were analyzed by comparing the somatic mutation data from the TCGA database using the R package "maftools". The cosine similarity method was used to extract the difference between the obtained mutational signature and the mutation database (COSMIC V2). The differential methylation-driven genes were identified by the methylation data (TCGA-LIHC Illumina Human

Methylation 450) from the TCGA database using the MethylMix package. A waterfall plot and heatmap were drawn by the "Complex HeatMap" R package to analyze the significantly variation CNV segments (alternation frequency >0.3) between two non-apoptotic RCD subtypes.

Generation of non-apoptotic RCD-related signature in HCC patients

The relationship between non-apoptotic regulated cell death (RCD)-related mRNAs and overall survival (OS) in HCC patients was investigated using univariate Cox regression analysis. Lasso Cox regression and multiple stepwise regression analysis were performed only for mRNAs with statistically significant differences. Afterward, multiple regression coefficients were used to establish non-apoptotic RCD-related signature (RCDRS) evaluation panels based on four genes (PLOD2, G6PD, FTCD, and ADH4). Using the coefficients of four enrolling genes obtained from the linear regression model, RCDRS score were calculated according to the following formula:

$$\text{RCDRS score} = \sum_{i=1}^{n} \text{Coei} * \text{Expi}$$

The Coei and Expi represented the gene expression coefficients and the corresponding gene expression levels, respectively. RCDRS scores were computed for patients with HCC, and subsequently, they were categorized into high- and low-RCDRS groups based on a cut-off value determined using the survminer package in R. The OS efficiency of patients in the two groups was then evaluated through Kaplan-Meier analysis. The GSE116174 cohort served as the independently validated cohort to verify the value of this RCDRS panel.

Prediction of chemotherapeutic responses and potential small molecule drugs

To predict the chemotherapy response in HCC patients, the R package "pRRophetic"[59] was employed. Ridge regression was utilized to estimate the half maximal inhibitory concentration (IC50), and the accuracy of the predictions was evaluated through a 10-fold cross-validation using the GDSC training set.[60] Potential small molecule drugs for HCC patients' treatment were screened from the Connection graph (CMap) database by eXtreme Sum (XSum) algorithm.[61]

HCC patients tissue samples collection

20 pairs of HCC tumor tissues and the corresponding matched adjacent normal tissues were collected from all primary HCC patients undergoing surgery between January 2021 and June 2022 in Department of hepatobiliary and pancreatic surgery of Zhongnan Hospital of Wuhan University. HCC was diagnosed according to the practice guideline by American Association for the Study of Liver Diseases (AASLD).[62] All participants signed informed consent, none received local, systemic treatment before surgery, and tissues collected from the surgery room were immediately stored in liquid nitrogen tanks. This study was approved by the Medical Ethics Committee of Zhongnan Hospital of Wuhan University (Kelun [2021007-1K]).

Quantitative real-time PCR (qRT-PCR) analysis

Total RNAs were extracted from tissues with Trizol reagent (Thermo Fisher Scientific, USA), and then reverse transcribed cDNA was generated by the HiFiScript gDNA Removal RT MasterMix kit (CWBIO, China). The qRT-PCR was performed using the CFX Connect real-time PCR system (Bio-Rad, USA) and MagicSYBR Mixture kits (CWBIO, China). The GAPDH was used as a control in PCR runs. And the date was analyzed by the $2^{-\Delta\Delta Ct}$ method.[63] All experiments were performed in triplicate independent. The gene-specific primer sequences are listed as follows in Table S3.

Immunohistochemistry staining

Immunohistochemical staining was performed according to the standard laboratory procedures. The tissue samples were fixed with paraformaldehyde, dehydrated with different concentrations of ethanol, and then embedded in liquid paraffin to make 5 μm thick sections. All these reagents were provided by the Department of pathology, Zhongnan Hospital. Slides were nonspecifically covered with sodium citrate antigen repair solution (pH 6.0) and 3% BSA before sequential incubation with anti-PLOD2 antibody (21214-1-AP, Proteintech), anti-G6PD antibody (25413-1-AP, Proteintech), anti-FTCD antibody (21959-1-AP, Proteintech) and anti-ADH4 antibody (16474-1-AP, Proteintech) at 4°C overnight. Then incubated with HRP-conjugated secondary antibodies, followed by the addition of 3,3'-diaminobenzidine and hematoxylin for chromogenic reaction, and the positive cells were observed and counted under a slice scanner (Pannoramic SCAN,3DHISTECH CaseViewer, Hungary). The immunohistochemical staining images all originated from the same patient sample.

Multiplexed immunofluorescence staining

The expression of PLOD2, G6PD, FTCD, and ADH4 in HCC tissue microarray (D181Lv01, bioaitech, China) were detected by multiplexed immunofluorescence staining. Multiplexed immunofluorescence staining was conducted as previously described.[64] Briefly, the slides were deparaffinized and dehydrated, antigen retrieval, and endogenous peroxidase and antigen blocking followed by sequential incubation with corresponding specific antibodies, and then tyramide signal amplification (TSA) systems was performed for multiplexed immunofluorescence staining, and nucleus DNA was counterstained with DAPI (Biosharp, Guangzhou, China) and then observed under a slice scanner (Pannoramic SCAN,3DHISTECH CaseViewer, Hungary) and the positive cells were counted.

QUANTIFICATION AND STATISTICAL ANALYSIS

All statistical analyses were carried out using R 4.1.1 software. Differences among three or more groups were assessed using the Kruskal-Wallis test. The consensus clustering method was applied to cluster non-apoptotic regulated cell death (RCD), and Kaplan-Meier analysis was employed to generate survival curves for prognostic analysis of HCC patients. Fisher's exact test was used to examine the relationship between clinical characteristics and the two clusters. Univariate and multivariate Cox regression analyses were performed to investigate the association between RCDRS and the prognosis of HCC patients. Statistical significance was defined as $p < 0.05$. *$p < 0.05$, **$p < 0.01$, ***$p < 0.001$.

Additional resources

This study did not generate additional data.